paper submitted for the proceedings of the 2016 ESA Living Planet Symposium
held in Prague, Czech Republic, 9-13 May 2016, ESA Special Publication SP-740

ACOLITE FOR SENTINEL-2: AQUATIC APPLICATIONS OF MSI IMAGERY

Quinten Vanhellemont[(1)] and Kevin Ruddick[(1)]

[(1)]Royal Belgian Institute for Natural Sciences, Operational Directorate Natural Environment, Gulledelle 100, 1200 Brussels, Belgium, e-mail: quinten.vanhellemont@naturalsciences.be

ABSTRACT

Here we present the application of Sentinel-2 imagery for coastal and inland waters, and the ACOLITE processor and atmospheric correction developed in the EC-FP7 HIGHROC project. The MultiSpectral Imager (MSI) on board of Sentinel-2 has a pair of 20 m SWIR bands at 1.6 and 2.2 µm, allowing for a robust image-based atmospheric correction, even over extremely turbid waters. One of the main advantages of Sentinel-2 over Landsat-8 is the inclusion of a 20 m resolution red-edge band at around 705 nm, allowing for the determination of chlorophyll a absorption in turbid and productive waters, where open ocean blue-green ratio algorithms fail. MSI has red (665 nm) and NIR (842 nm) bands at 10 m spatial resolution, allowing for the retrieval of turbidity or suspended particulate matter concentration, even in narrow inlets and ports. This makes it an invaluable dataset for validating sediment transport models that are needed for optimization of dredging operations and coastal defence around ports. The spectral, spatial, and radiometric resolutions of Sentinel-2 and Landsat-8 are compared and discussed. For many aquatic applications these missions will typically be combined as a virtual constellation to improve temporal coverage. We provide here one example of using both sensors to track a cyanobacterial bloom in an Australian lake.

1. Introduction

The first satellite of the Sentinel-2 constellation, Sentinel-2A (S2A) was successfully launched on the 23rd of June 2015. It has on board the MultiSpectral Imager (MSI), an optical imager with 13 spectral bands spanning from the blue to the shortwave infrared (SWIR) with 10, 20, or 60 m ground resolution. As previously demonstrated with imagery at 30 m resolution from the Operational Land Imager (OLI) lauched in 2013 on board of Landsat-8 (L8), many human activities in coastal waters such as offshore construction and dredging, and their impacts, are spatially resolved at these resolutions (Vanhellemont and Ruddick, 2015, 2014a). Both the Landsat-8 and Sentinel-2 missions are land-oriented missions, but due to their improved quality compared to older missions (in terms of signal-to-noise ratio, SNR) they have proven to be useful for estimation of water reflectance and hence mapping of water quality parameters. Thanks to the free dissemination of data from both systems, we are entering a new era of high resolution water colour remote sensing.

In this paper, we show a first evaluation of the MultiSpectral Imager on Sentinel-2 (S2/MSI) for aquatic remote sensing applications, and compare it with the Operational Land Imager on Landsat-8 (L8/OLI) in terms of (1) spectral band sets, (2) noise specification, and (3) spatial resolution. We also present an update to the ACOLITE atmospheric correction and processor that now supports processing of both Landsat-8 and Sentinel-2, and is available to the public at (https://odnature.naturalsciences.be/remsem/acolite-forum/).

2. Methods and Results

For aquatic remote sensing applications, the atmospheric correction is a crucial step. ACOLITE aims to make this step robust and easy to use for high resolution satellite data. In general ACOLITE performs an atmospheric correction in two steps: (1) a Rayleigh correction for scattering by air molecules, using a Look-Up Table generated using 6SV(Vermote et al., 2006), and (2) an aerosol correction based on the assumption of black SWIR bands over water caused by the extremely high pure-water absorption, and an exponential spectrum for multiple scattering aerosol reflectance. ACOLITE outputs water-leaving radiance reflectances, hereafter called water reflectances (ρ_w), in all visible and NIR bands, and can compute multiple other parameters. For a complete overview of the atmospheric correction, the reader is referred to (Vanhellemont and Ruddick, 2015, 2014a). Updates to ACOLITE specifically for Sentinel-2 are described below.

2.1. ACOLITE processing of Sentinel-2 data

2.1.1. SAFE format

Sentinel-2 L1C scenes in the SAFE format contain orthorectified, geolocated and radiometrically calibrated top-of-atmosphere reflectances in Universal Transverse Mercator (UTM) projection with the WGS84 datum. A single L1C scene can contain multiple granules (sub-tiles), and can potentially extending over two UTM zones. As of now, ACOLITE supports the processing of full L1C scenes and individual granules. If a L1C scene is provided, each granule will be processed sequentially. When a region of interest (ROI) is specified, in terms of a box in latitude and longitude, each granule will be checked for coverage and cropped and processed if needed. If the ROI spans multiple granules within the same UTM zone, ACOLITE supports the automatic stitching together of data from the different granules to a single output file. Reprojection of data from adjacent UTM zones is planned for a future update, which will be announced via the ACOLITE web site.

2.1.2. Spatial resolution

MSI has spectral bands at different spatial resolutions, 10, 20 and 60 m (see Table 1). ACOLITE converts the bands internally to the same (user-specified) resolution. For bands at lower resolution than the processing resolution, values are replicated by nearest neighbour resampling, i.e. no new pixel values are computed, and for bands at higher resolution, pixels are spatially mean averaged. By default the 10 m grid is used, which means the values from the 20 and 60 m bands are replicated 4 and 36 times to form a 10 m grid.

2.1.3. Masking of non-water pixels

After Rayleigh correction, a non-water masking is performed to exclude land, clouds, glint and objects such as boats from further processing. The masking is performed using a threshold of 2.15% on the 1.6 µm band, which excludes most of the non-water pixels, but can miss cloud and mountain shadows, medium sun glint and thin clouds. This problem is however not unique to Sentinel-2 data and is the topic of on-going research (Pringle et al., 2015). The masking uses data from a 20 m resolution band, but is performed at the selected processing resolution.

2.1.4. Noise reduction of the aerosol correction bands

The SWIR bands at 1.6 and 2.2 µm are used by default for the aerosol correction, as they should be black over all water types. Due to the low signal at these long wavelengths, the digitization in the L1C files (1/10000), and the relatively low signal-to-noise ratio of MSI, a spatial smoothing filtering for these bands is needed. Typically aerosol type and reflectance will vary spatially and temporally, but generally not at the pixel length scales considered here. The mean spatial averaging is performed after the masking described above, to exclude bright SWIR pixels that will otherwise influence the surrounding dark (water) pixels. An optional spatial dilation of the mask can be performed to further exclude mixed or dubious pixels. The dilated mask can be filled using the median reflectance observed over water pixels, to further reduce the impact of missed or mixed brighter pixels around the masked area. The spatial filtering is illustrated in Figure 1, which shows a part of Lake Balaton, and ACOLITE outputs with fixed aerosol type (F) and variable aerosol type, with (V-32) and without (V) smoothing of the SWIR bands over an extent of 320 m. Transects in Figure 2 shows the signal variability and noise at short length scales. Smoothing of the SWIR bands allows the use of a variable aerosol type, and greatly improves the noise level in the output products. The smoothing option is now also available for OLI, which further improves ACOLITE performance when processing with a variable aerosol type.

2.2. Comparison of L8/OLI and S2/MSI

2.2.1. Spatial resolution

S2/MSI and L8/OLI have bands at different spatial resolution as detailed in Table 1 and Table 2. S2/MSI has a blue/green/red/NIR band at 10 m resolution, and compared to L8/OLI is has additional NIR/SWIR bands at 20 m resolution. S2/MSI also has a set of 60 m bands intended for atmospheric correction and masking over land: its shortest blue band, water vapour and cirrus bands. L8/OLI has 8 bands at 30 m spatial resolution, and a panchromatic band at 15 m resolution.

For aquatic applications, the improved resolution with regards to L8/OLI of the 10 m VNIR bands allows for a better separation of small scale features, such as those caused by human activities or constructions (dredger plumes, tidal sediment wakes) and allows for the observation within smaller inlets. In Figure 3, a visual comparison is made of the relatively narrow tidal sediment wakes of the Dumbarton Bridges in South San Francisco Bay. On the L8/OLI image at 30 m resolution, these tidal wakes are not well resolved or spatially separated. The separation of the wakes is improved for L8 after pan-sharpening (Vanhellemont and Ruddick, 2014b), but the sharpening procedure introduces artefacts, especially around bright non-water pixels. S2/MSI at 10 m shows well separated wakes and even resolves some of the finer turbulent features within the wakes. Although MSI data can be rather noisy at native resolution, we recommend in first instance not to resample the high resolution bands for noise reduction, as the spatial resolution is one of its strengths. In many bright coastal waters the high resolution bands will give adequate performance.

2.2.1. Noise specification

The pre-launch signal-to-noise (SNR) performance of L8/OLI is provided at two reference radiances (L_{ref}); a 'typical' and a 'high' reference radiance (Irons et al., 2012). The 'typical' L_{ref} are comparable to the top-of-atmosphere radiances encountered over water pixels (Hu et al., 2012; Vanhellemont and Ruddick, 2015). The S2/MSI SNR specification is given at L_{ref} values comparable to the 'high' L_{ref} of L8/OLI for the visible and NIR (VNIR) bands and to the 'typical' L_{ref} for the shortwave-infrared (SWIR) bands. Therefore the comparison here is made using the 'high' L_{ref} SNR values for the VNIR and the 'typical' L_{ref} for the SWIR bands (see Table 1 and Table 2 for an overview). It is not yet known how the MSI instrument performs at the lower radiances typically encountered over water pixels (similar to the 'typical' L_{ref} for L8/OLI).

The pre-launch characterization of L8/OLI, 50-100% higher than its specification (Irons et al., 2012), shows that its SNR is much higher than the specification of S2/MSI The SNR values of MSI are provided at native resolution, and after aggregation of the 10 m pixels to Landsat-like resolution of 30 m resolution (9 pixels) SNR will obviously improve by a factor 3. For the SWIR bands used in the atmospheric correction, S2/MSI and L8/OLI have a similar L_{ref}, but the former has about 1/3 of the SNR specification of the latter. To reduce the noise introduced by the atmospheric correction for S2/MSI, we prefer the application of a mean average filtering to the SWIR bands (see 2.1.4).

2.2.2. Spectral band set and chlorophyll algorithms

An overview of the S2/MSI and L8/OLI band sets is given in Table 1 and Table 2. Eight of the bands on the two imagers are more or less directly comparable in terms of band centre wavelength, with L8/OLI in general having wider bands in the VNIR. In general, parameters that can be retrieved with L8/OLI can also be retrieved with S2/MSI, at higher resolution with some impact on the product noise (see above). The main differences in the band set are the addition on S2/MSI of a red-edge band at 705 nm, three additional NIR bands (740, 775, 842 nm) and a water vapour band at 940 nm.

For aquatic applications (indubitably also for terrestrial applications) the 705 nm band provides a much needed reference point for retrieving chlorophyll-a absorption at 665 nm and thus can be used for estimating the chlorophyll-a concentration in turbid and productive waters. Several algorithms exist that exploit information in this spectral region, typically designed for MERIS or hyperspectral data (e.g. Gilerson et al., 2010; Gons et al., 2005). (Gons et al., 2005) provide a method to retrieve the phytoplankton absorption. This is here replicated with no recalibration from MERIS to S2/MSI since we found only small differences between simulated reflectance spectra convoluted to the relative response functions of MERIS and MSI (not shown here). First backscatter (in m^{-1}) is estimated from the water reflectance at 775 nm (778 nm for MERIS):

$$b_b = \frac{1.61 \cdot \rho_w 775}{0.082 - 0.6 \cdot \rho_w 775} \quad (1)$$

The retrieved b_b and a band ratio between ρ_w at 705 (709 nm on MERIS) and 665 nm is used to retrieve the phytoplankton absorption at 665 nm (a_ϕ^{665} in m^{-1}):

$$a_\phi^{665} = \left[(0.70 + b_b) \cdot \left(\frac{\rho_w 705}{\rho_w 655}\right) - 0.40 - {b_b}^{1.05}\right] \quad (2)$$

Chlorophyll a concentration (mg m^{-3}) can then be retrieved assuming a certain specific absorption coefficient (set by (Gons et al., 2005) to a_ϕ^* = 0.014 m^2 mg^{-1}):

$$chla = \frac{a_\phi}{a_\phi^*} \quad (3)$$

Both L8/OLI and S2/MSI have appropriate bands for the traditional 'ocean chlorophyll' (OC) blue-green ratio algorithms to retrieve chlorophyll a concentration:

$$chla = 10\hat{}(a_0 + a_1 \cdot R + a_2 \cdot R^2 + a_3 \cdot R^3 + a_4 \cdot R^4) \quad (4)$$

where R is the logarithm of the ratio of maximum blue reflectance to green reflectance. This algorithm was calibrated for L8/OLI by (Franz et al., 2015) and this calibration was applied here for OLI and MSI in the 3 band configuration (~440, ~490 and ~560 nm) with a_{0-4} of 0.2412, -2.0546, 1.1776, -0.5538, and -0.4570.

While the necessary spectral bands exist for both the red-edge and OC algorithms it is important to note that application of these algorithms to S2/MSI data is subject to performance limitations of the algorithms related to the natural variability of a_ϕ^*, and the impact of CDOM and non-algal particles (NAP). Additional limitations specific to Sentinel-2 can arise, due to its relatively wide bands, low SNR and lack of vicarious calibration.

2.3. Virtual constellation of L8 and S2

A case study is presented here using the virtual constellation of L8/OLI and S2/MSI, following a cyanobacterial bloom in the Murray River, Australia. Rayleigh-corrected RGB composites of Lake Mulwala from S2/MSI and L8/OLI images taken 13 days apart, show the green colouration of the lake water due to an intense bloom of cyanobacteria (Figure 4). Although the images were taken two weeks apart, spectra from MSI and OLI compare well, showing a strong reflectance peak in the green (left panel of Figure 5). The MSI spectrum clearly shows the value of the red-edge band that allows for the quantification of the red band absorption by chlorophyll a, which is impossible using OLI by itself. Time-series of 8 L8/OLI images and 4 S2/MSI images from September 2015 onwards reveal a relatively constant blue (483/497 nm for OLI/MSI), green (560/561 nm) and red (655/664 nm) reflectance during the last part of 2015 (middle panel of Figure 5). In early 2016, corresponding to the start of the cyanobacterial bloom, the green reflectance increases, while the red reflectance decreases and the blue reflectance remains at a comparable level to the end of

2015. S2/MSI images reveal a high reflectance in the red-edge band at 704 nm, allowing the attribution of the decrease in red reflectance to an increased chlorophyll a absorption. Note that both the blue/green ratio and the red-edge algorithms are able to track the bloom reasonably well (right panel of Figure 5), probably because the non-algal suspended matter concentration in the lake is relatively low and does not significantly impact the blue-to-green ratio.

3. Conclusions

The MultiSpectral Imager (MSI) on Sentinel-2 (S2) has the potential to bring a number of new applications to coastal and inland water quality management. Thanks to its high resolution VNIR bands (10 m) existing applications such as turbidity mapping can be improved and extended to other smaller or narrower water bodies. As demonstrated here, thanks to its red-edge band at 705 nm, S2 imagery can be used to detect chlorophyll a absorption in the red band (665 nm) and hence mapping of chlorophyll a concentration at 20 m resolution is now a possibility. We have introduced here the atmospheric correction of Sentinel-2 imagery using an updated version of the ACOLITE processor, now publicly available. At this point we recommend a moving average filter on the SWIR bands used for aerosol correction, but to leave the other bands at their native resolution or upsampled to 10 m, which will allow proper evaluation of potential applications and the noise level in the products.

The comparison of S2/MSI to the Operational Land Imager (OLI) on board of Landsat-8 (L8) shows the latter has the advantage of higher SNR in its 30 m bands, with potential for sharpening using the 15 m panchromatic band. Due to the similar band sets, many parameters can be derived from both sensors, apart from the ones related to red band chlorophyll a absorption. L8 also has on board the two-band Thermal Infrared Sensor (TIRS) that allows for lake and sea surface temperature retrieval, better detection of clouds, as well as the estimation of cloud height. Due to the relatively low revisit time of the S2 (10 days with one unit, 5 days with two) and L8 missions (16 days), they have to be seen as a virtual constellation for observing the rapidly varying aquatic systems. Not only can combining the two systems improve temporal coverage, but MSI observations can also be used to interpret trends observed by OLI. This was here demonstrated using the red-edge band on MSI to explain the decrease in the red spectral region observed over multiple OLI images.

Acknowledgements
This work was performed for the European Community's Seventh Framework Programme (FP7/2007-2013) under grant agreement n° 606797 (HIGHROC project). USGS and ESA are thanked for the satellite data. Sentinel-2 imagery was acquired in the SAFE file format via the Copernicus Sentinels Scientific Data Hub and Landsat-8 imagery was acquired in the GeoTIFF format via USGS.

4. References

Drusch, M., Gascon, F., Berger, M., 2010. GMES Sentinel-2 mission requirements document. ESA EOP-SM1163MR-Dr2 42.

Franz, B.A., Bailey, S.W., Kuring, N., Werdell, P.J., 2015. Ocean color measurements with the Operational Land Imager on Landsat-8: implementation and evaluation in SeaDAS. J. Appl. Remote Sens. 9, 096070–096070.

Gilerson, A.A., Gitelson, A.A., Zhou, J., Gurlin, D., Moses, W., Ioannou, I., Ahmed, S.A., 2010. Algorithms for remote estimation of chlorophyll-a in coastal and inland waters using red and near infrared bands. Opt. Express 18, 24109–24125.

Gons, H.J., Rijkeboer, M., Ruddick, K.G., 2005. Effect of a waveband shift on chlorophyll retrieval from MERIS imagery of inland and coastal waters. J. Plankton Res. 27, 125–127.

Hu, C., Feng, L., Lee, Z., Davis, C.O., Mannino, A., McClain, C.R., Franz, B.A., 2012. Dynamic range and sensitivity requirements of satellite ocean color sensors: learning from the past. Appl. Opt. 51, 6045–6062.

Irons, J.R., Dwyer, J.L., Barsi, J.A., 2012. The next Landsat satellite: The Landsat Data Continuity Mission. Remote Sens. Environ. 122, 11–21.

Pringle, N., Vanhellemont, Q., Ruddick, K., 2015. Cloud and cloud shadow identification for MERIS and Sentinel-3/OLCI. ESA Spec. Publ. 734.

Vanhellemont, Q., Ruddick, K., 2015. Advantages of high quality SWIR bands for ocean colour processing: examples from Landsat-8. Remote Sens. Environ. 161, 89–106. doi:10.1016/j.rse.2015.02.007

Vanhellemont, Q., Ruddick, K., 2014a. Turbid wakes associated with offshore wind turbines observed with Landsat 8. Remote Sens. Environ. 145, 105–115. doi:10.1016/j.rse.2014.01.009

Vanhellemont, Q., Ruddick, K., 2014b. Landsat-8 as a Precursor to Sentinel-2: Observations of Human Impacts in Coastal Waters., in: ESA Special Publication SP-726. Presented at the 2014 European Space Agency Sentinel-2 for Science Workshop, Frascati.

Vermote, E., Tanré, D., Deuzé, J., Herman, M., Morcrette, J., Kotchenova, S., 2006. Second simulation of a satellite signal in the solar spectrum-vector (6SV). 6S User Guide Version 3..

Table 1 Bands of the MultiSpectral Imager (MSI) on Sentinel-2, with central wavelength and width, ground sampling distance (GSD), signal-to-noise ratio (SNR) at reference radiance (Drusch et al., 2010).

Band	Wavelength (nm)	Width (nm)	GSD (m)	SNR at reference L	reference L (W m^{-2} sr^{-1} μm^{-1})
1	443	20	60	129	129.0
2	490	65	10	154	128.0
3	560	35	10	168	128.0
4	665	30	10	142	108.0
5	705	15	20	117	74.5
6	740	15	20	89	68.0
7	775	20	20	105	67.0
8	842	115	10	172	103.0
8b	865	20	20	72	52.5
9	940	20	60	114	9.0
10	1375	20	60	50	6.0
11	1610	90	20	100	4.0
12	2190	180	20	100	1.5

Table 2 Bands of the Operational Land Imager (OLI) on Landsat-8, with wavelength range, ground sampling distance (GSD), signal-to-noise ratio (SNR) at 'high' reference radiance for the VNIR bands and at 'typical' reference radiance (underlined) for the SWIR bands (Irons et al., 2012).

Band	Name	Wavelength (nm)	GSD (m)	SNR at reference L	reference L (W m^{-2} sr^{-1} μm^{-1})
1	Coastal/Aerosol	433–453	30	607	190.0
2	Blue	450–515	30	1127	190.0
3	Green	525–600	30	1213	194.0
4	Red	630–680	30	945	150.0
5	NIR	845–885	30	1009	150.0
6	SWIR 1	1560–1660	30	261	4.0
7	SWIR 2	2100–2300	30	326	1.7
8	PAN	500–680	15	440	190.0
9	CIRRUS	1360–1390	30	162	6.0

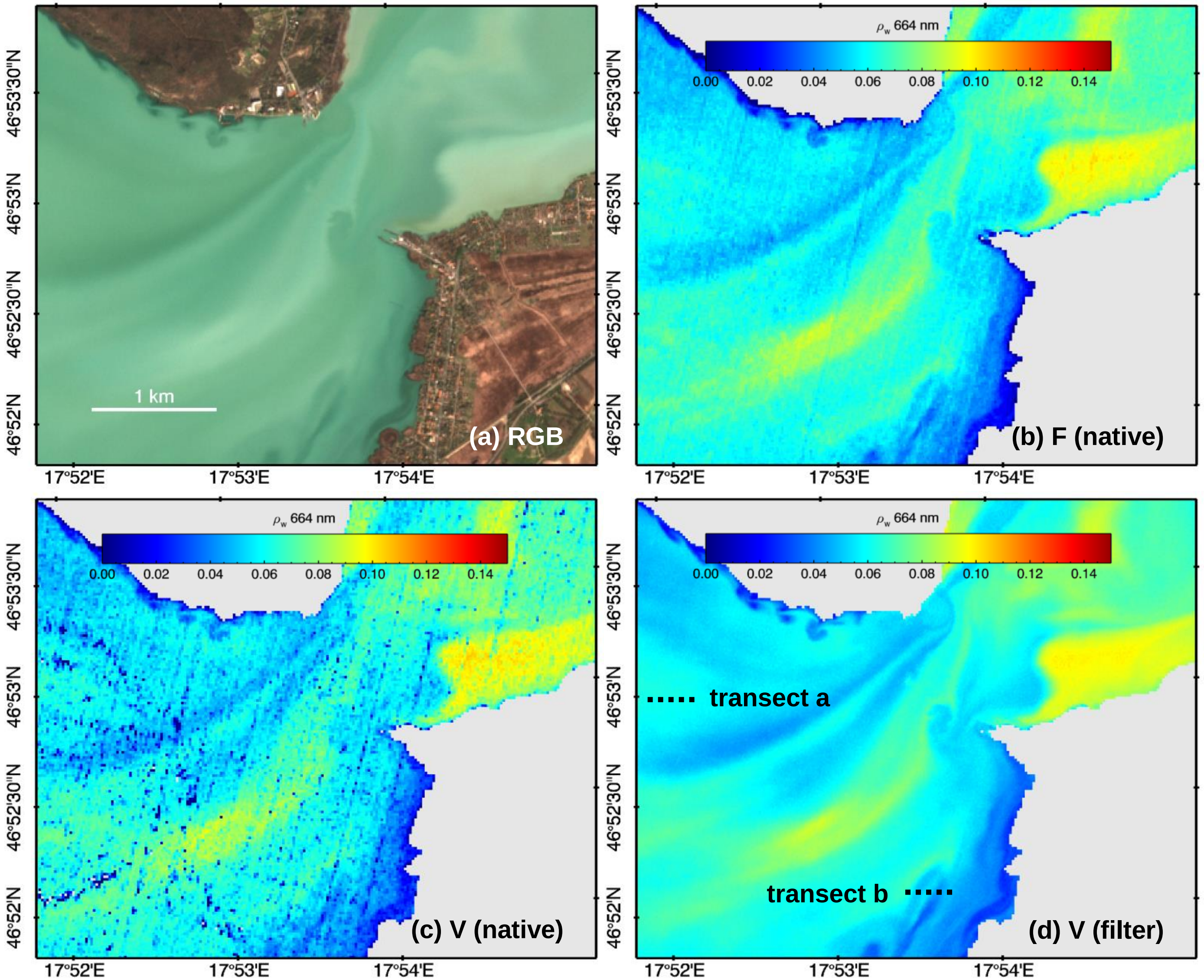

Figure 1 (a) Rayleigh corrected RGB composite of the S2/MSI 10 m bands (665/560/490 nm), showing a part of Lake Balaton on 2016-03-14. Water reflectance at 665 nm is shown, without resampling of the SWIR bands for (b) a fixed sub-scene aerosol type (epsilon) and (c) a per-pixel variable epsilon, and (d) after mean averaging of the SWIR bands over 320 m, using a variable epsilon. The black dashed lines indicate the two transects shown in Figure 2.

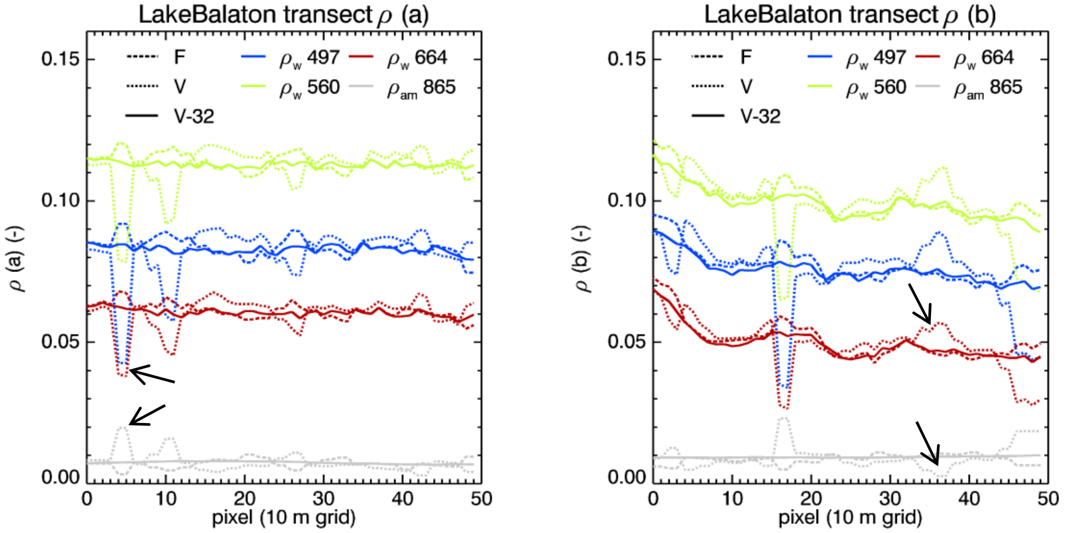

Figure 2 Two transects from Figure 1, with (a) an almost invariant water signal, and (b) some features in the water. Water reflectances (ρ_w) from the three high resolution bands (blue = 490 nm, green = 560 nm and red = 665 nm) and the multiple-scattering aerosol reflectance (ρ_{am}) at 865 nm (grey) are plotted for three processing options: (long dashed) F = fixed aerosol type, (short dashed) V = variable aerosol type and (solid) V-32 = variable aerosol type with mean averaged SWIR bands. The impact of anomalous reflectance (noise) in one or two of the SWIR bands can be seen on both the ρ_w and ρ_{am} (black arrows), especially for the V method. The coefficient of variation (CV=standard deviation / mean) is here used to estimate the noise from the stable transect. The CV in $\rho_{w\ 664}$ (the 10 m band with lowest SNR and here also lowest signal) is 4%, 10% and 2% for F/V/V-32, with a CV in $\rho_{am\ 865}$ of 24%, 49% and 6%.

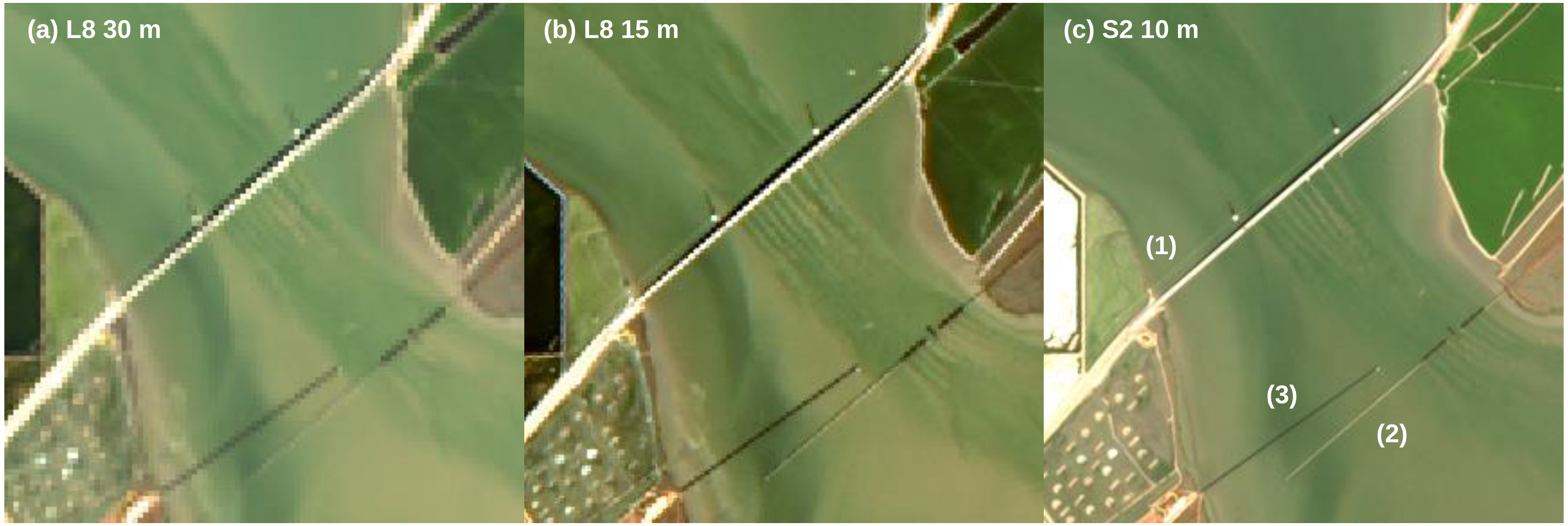

Figure 3 A comparison of the different resolutions of Landsat-8 (L8) and Sentinel-2 (S2), using Rayleigh-corrected RGB composites over the Dumbarton Highway (1) and Railway (2) bridges, and the Hetch Hetchy Aquaduct (3) in South San Francisco Bay. (a) Landsat-8 (2015-10-31) at 30 m resolution, (b) the same Landsat-8 image, sharpened using the 15 m panchromatic band, and (c) Sentinel-2 (2015-09-15) at 10 m resolution. L8 and S2 imagery was acquired at similar tidal state but on different dates at similar overpass times (note the length of the bridge pylon shadows, showing the lower sun elevation at the later acquired L8 image).

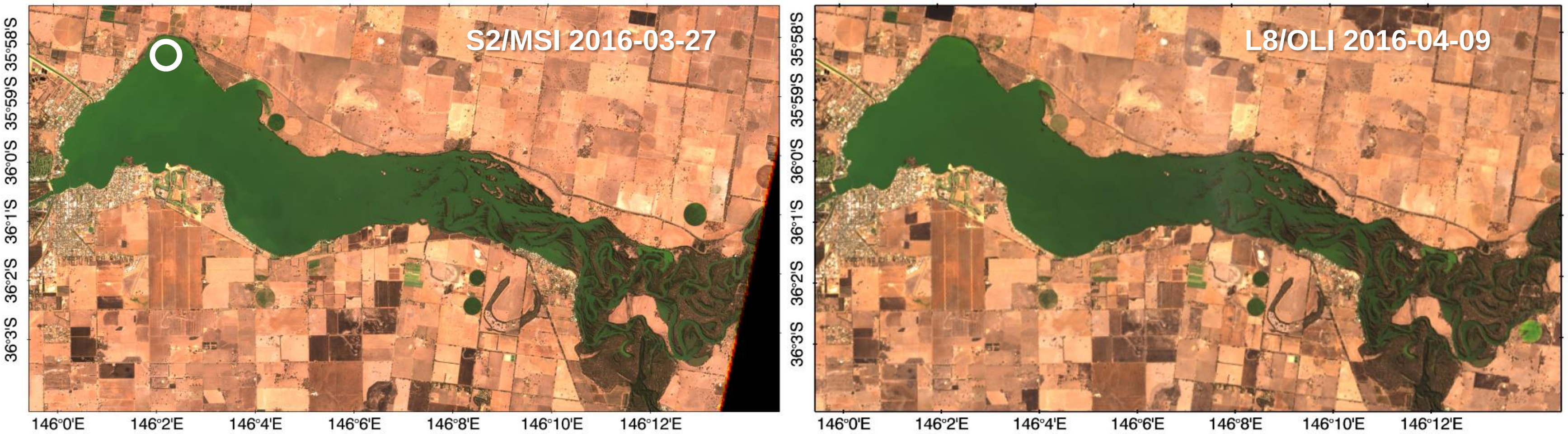

Figure 4 A cyanobacterial bloom in Lake Mulwala (Victoria, Australia) observed by Sentinel-2/MSI on 2016-03-27 (left) and Landsat-8/OLI on 2016-04-09 (right), Rayleigh-corrected RGB composites using bands at 10 m (MSI: 665/560/490 nm) and 30 m (OLI: 655/561/483 nm) resolution. Water reflectance spectra as well as time-series from both sensors are given in Figure 5 for a point in the bay indicated by the white circle.

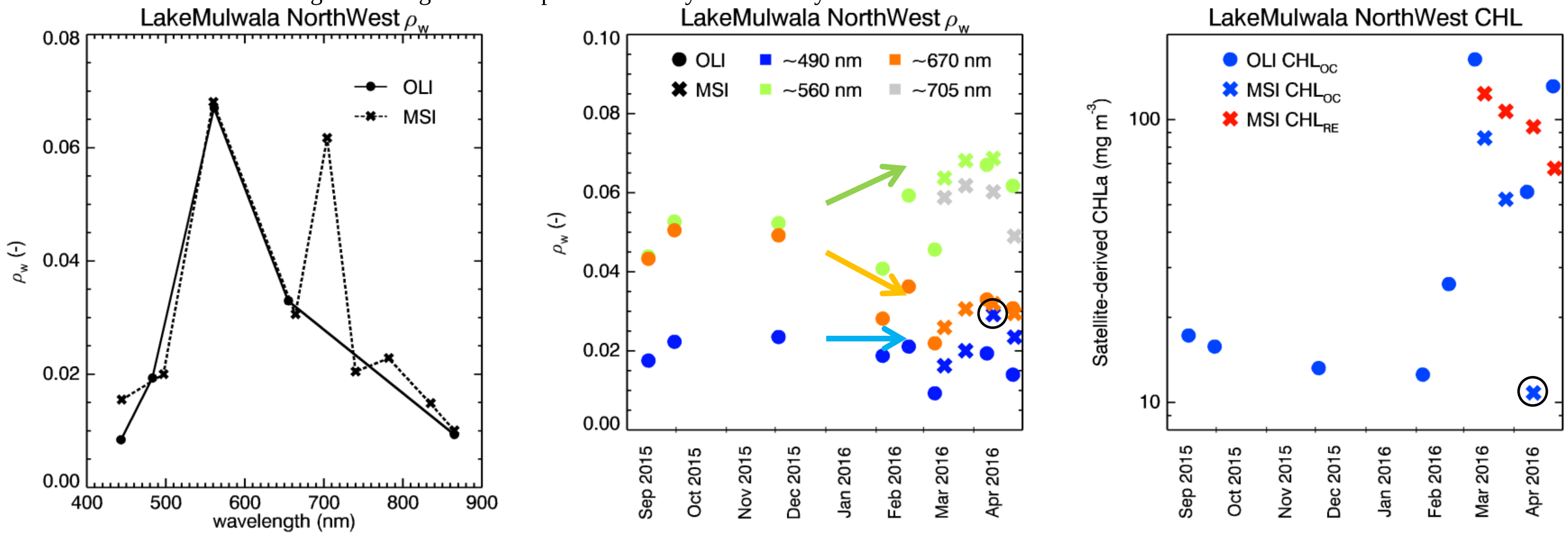

Figure 5 Water reflectance (ρ_w) spectra from MSI (on 2016-03-27) and OLI (on 2016-04-09) for a point in the northernmost bay in Lake Mulwala (left), and time-series of ρ_w (middle) and chlorophyll a concentration from OC and red-edge (RE) algorithms (right). Values are the median of a 9x9 box. Note the decrease in red reflectance and the increase in green reflectance. Rather high blue reflectance was observed by S2/MSI on 13th of April, impacting the OC algorithm (black circles).